**DINAMIKA TEKNIK SIPIL**
**MAJALAH ILMIAH TEKNIK SIPIL**
**Volume 17, Nomor 1, Juli 2024, Halaman 16-24**
**p-ISSN: 1411-8904, e-ISSN: 2828-2876**
**Tersedia online di https://journals.ums.ac.id/index.php/DTS/index**

# FORECASTING A LONG-TERM LANDSLIDE HAZARD IN PAWEDEN AND KALILUNJAR SUB-DISTRICT, BANJARNEGARA, INDONESIA

**Diah Valentina Lestari**[1*], **Gayuh Aji Prasetyaningtiyas**[2]
[1]School of Civil and Environmental Engineering, Nanyang Technological University,
50 Nanyang Avenue, Singapore 639798
[2]Department of Civil Engineering, Faculty of Engineering, Universitas Muhammadiyah Surakarta,
Jl. A. Yani Tromol Pos 1 Pabelan, Kartasura, Surakarta, Indonesia, Post Code 57162
[*]Email: valentina.diah@ntu.edu.sg
Submitted: 30/06/2024 Revised: 19/07/2024 Accepted: 20/07/2024

**Abstract**

*Climate change has been a global issue for the past decades. It has impacted numerous aspects in landslide, particularly in the slope stability. The soil mass rupture leads to damage to infrastructure and death. Thus, any prevention is urgently needed to minimize the risk. Forecasting the hazards is part of disaster management. The Initial step of this action is forecasting the rainfall due to climate change for the next 20 years since 2010, given that most of the landslide hazards in Paweden and Kalilunjar are triggered by rainfall. This study uses CORDEX-SEA to obtain the rainfall forecasting data as the input to simulate the slope stability. The rainfall seepage is performed to obtain slope safety factor by using Geo-studio. Two chosen sub-districts in Banjarnegara, Paweden and Kalilunjar, are expected to experience more extreme daily rainfall by the end of 2030 compared to 2010 conditions. This study also shows that all rainfall cases trigger a slope failure (FS<1.2). This study is expected to support the local government in deciding the next hazard mitigation plan.*

***Keywords**: Rainfall, Slope Stability, Seepage, Paweden, Kalilunjar*

## 1. INTRODUCTION

As the atmosphere warms under a global warming scenario, the global climate model's (GCM) projection implies a wet gets wetter and dry gets drier (WWDD) paradigm (Held and Soden, 2006). However, the WWDD pattern is not consistent over the land areas with about 20% of global land areas projected to experience WWDD meanwhile 29% of global land areas experiencing an opposite pattern in the future (Yang et al., 2019, Zaitchik et al., 2023). Based on a GCM projection, Indonesia shows a tendency to be one of the wet regions along with most of the countries in Southeast Asia and the other tropical regions. Overall, GCM projects an increase in rainfall intensity over the wet region in the future (Weidman, 2021). Not only rainfall in general, El Niño-Southern Oscillation (ENSO) as the main climate variability in the Equatorial Pacific is expected to partially contribute to rainfall intensification in the future (Deser et al., 2010, Yun et al., 2021). During its La Niña condition, ENSO influences the wet season's rainfall variabilities in Indonesia which also contributes to the future rainfall intensity in Indonesia (Hendrawan et al., 2019, McGregor et al., 2022, Nguyen-Thanh et al., 2023). With such changes in underlying conditions for Indonesian rainfall variabilities, it is likely that Indonesia will experience a wetter condition under global warming. Crozier (2010) summarized that both rainfall intensity and frequency are two potential parameters that may affect the slope stability and they lead to a change in landslide event frequency.

Annual landslides influence the social and economic loss in Banjarnegara, Indonesia. For decades, slope failure has been the major issue in this district. According to Prasetyaningtiyas et al. (2023), the majority of slope failure in Banjarnegara is triggered by rainfall. Karnawati et al. (2009) mention that landslides have been the national focus of the Indonesian government since 2005. Some previous studies reveal the hazard management in Banjarnegara district. Prasetyaningtiyas et al. (2024) conducted a field investigation and numerical modeling to understand the rainfall characteristics in Wanayasa-Karangkobar lane. The study shows that the rainfall duration provides a higher impact on slope instability rather than the rainfall intensity. Muntohar et al. (2017) state that the slope with inclination greater than 30° is prone to landslide after 3hr of heavy rainfall. A similar research held by Arrisaldi et al. (2021) suggests a threshold of rainfall in Kulonprogo based on landslide events in 5 years. However, those previous studies fail to provide a longer period of rainfall threshold using a climate model.

With intensified rainfall in Indonesia and the wet gets wetter (WW) paradigm under global warming, a high-resolution dataset provides an upgrade of spatial and temporal input. This is necessary to predict a regional slope stability which may provide a potential change in landslide activity in the future (Crozier, 2010). Emberson and Stanley (2021) investigate NASA Landslide Hazard Assessment for Situational Awareness (LHASA) model on landslide exposure from the observed La Niña condition. They imply that La Niña leads to a greater impact on the landslide in Indonesia, indicating the importance of large-scale climate variabilities in improving the landslide hazard prediction and exposure. Also, this suggests the important usage of climate models.

In addition, the use of gauge-adjusted satellite product shows no improvement in landslide prediction and its regional early warning system in Progo Catchment, Java, Indonesia (Satyaningsih et al., 2023). A study demonstrates the use of downscaled GCM on projected downscaled rainfall lead to increase in landslide occurrence in China under representative concentration pathway (RCP) 8.5 scenario compared to the current climate (Lin et al., 2020). In this study, the use of downscaled GCM under Coordinated Regional Climate Downscaling Experiment–Southeast Asia (CORDEX-SEA) model is explored to assess the potential usage of climate model in regional landslide projection. This way, we may study the impact of long-term rainfall forecasting due to climate change. Next, the slope stability is simulated using a numerical model to understand the effect of rainfall characteristics on slope stability. The methodology of data selection and slope stability modeling is covered in Section 2. Section 3 provides a throghout discussion of each stage in determining the slope stabilities based Geostudio as well as the change in rainfall-based landslide under global warming. A brief conclusion of this study is presented in Section 4.

## 2. METHODOLOGY

### 2.1 Rainfall Variability

In this study, daily rainfall variability is assessed based on regional climate model (RCM) projection as a downscaled product from the global change model (GCM) with a finer horizontal resolution (0.22°×0.22°). A single ensemble CORDEX–SEA model is utilized to show the rainfall trends from 1971-2040 to avoid inter-model bias (Giorgi et al., 2009). With the least root mean square error among 11 RCMs in the CORDEX-SEA list, RCA4-CNRM-CM5 is chosen as a single model rainfall analysis during the historical/current climate (1971-2005) and future projection (2006-2040) (Nikulin et al., 2012, Nguyen et al., 2022).

Under an intermediate emission scenario, the rainfall is projected following the representative concentration pathway (RCP) 4.5 to analyze the climate change influence on the rainfall pattern. In addition, the daily mean dataset is chosen to represent the daily rainfall variability during the wet season (December-January; DJF). In this study, an area-mean method is applied to the daily accumulated rainfall during DJF from 1971-2040 within the area of analysis that covers both Paweden and Kalilunjar sub-district region at 7.26°-7.48°S & 109.5°-109.72°E (black-dashed box in Fig. 1).

### 2.2 Hourly Rainfall Input

The rainfall model has been established by using the daily rainfall data from 2010 to 2030. These data are categorized as the past (2010-2024) and forecasting period (2025-2030), respectively. Both categories are calculated as average rainfall. Since the rainfall data from CORDEX-SEA is the daily accumulated rainfall in mm/day units, hence the data is converted into mm/h. The duration per hour is determined by using previous work by Prasetyaningtiyas et al. (2024). The duration by Prasetyaningtiyas et al. (2024) is obtained by the offline rainfall station in Kalilunjar and satellite data. In this study, three different months are chosen (December, January, February). These months represent the highest rainfall in Banjarnegara Muntohar et al. (2017). The rainfall data from 2025 up to 2030 are useful to predict any landslide in the future based on the rainfall data.

### 2.3 Numerical model

The numerical model is carried out using GeoStudio under a plain strain model. The analysis contains two stages. The first stage is seepage modeling, where the model aims to analyze rainfall infiltration. This stage consists of steady-state and transient. The steady state is the initial condition prior to the rainfall event. Meanwhile, the transient is applied to analyze the condition during rainfall intensity.

The second stage is slope analysis. The objective of this phase is to analyze slope instability using Limit Equilibrium based on the Mohr-Coulomb criterion. The slip surface used grid and radius by Geo-Studio. The soil properties are obtained from a soil investigation report by the Soil laboratory at Diponegoro University (Laboratory, 2015). The slope model mimics existing conditions in the field. The slope geometry is attained by using a Global positioning system (GPS). A boundary condition is applied in the model. First boundary is the slope base is impermeable to prevent any water flow to the base, instead, the rainfall seepage and runoff flow to the slope surface or to the slope toe. The slope failure is established by Morgenstern price theory that follows (Fredlund, 1987):

$$\tau = c' + (u_a - u_w)tan\varphi^b + (\sigma - u_a)tan\varphi' \quad \mathbf{1}$$

where $\tau$ is the shear strength (kPa), ($u_a$-$u_w$ ) is the suction (kPa), $\phi^b$ is the angle indicating the rate of increase in shear strength with respect to a change in matric suction ($^o$). ($\sigma$-$u_a$) is net normal stress (kPa), $\phi'$ is the effective cohesion (kPa). The numerical is modeled by under plain strain and using circle slip surface to mimic existing condition.

## 3. RESULT AND DISCUSSION

### 3.1 Rainfall Changes under Global Warming

The wet season's daily rainfall variabilities in Paweden and Kalilunjar indicates a tendency towards less intense rainfall after 2010 (Fig. 2). With a less occurrence of rainfall with intensity greater than the 99th percentile of 1971-2040 rainfall in these regions by the end of 2040 (red line of Fig. 2). Indonesia is categorized as a WW region in general (Satyaningsih et al., 2023), but the area mean of rainfall over Paweden and Kalilunjar indicates a contrary pattern of future rainfall pattern (black line of Fig. 2).

However, the trend of annual mean rainfall is increased by around 23% in the future compared to the historical/current climate rainfall trend. This indicates that the annual mean rainfall is more suitable to represent the WW paradigm compared to the daily rainfall. Nevertheless, the occurrence of extreme rainfall (rainfall with intensity greater than 99th percentile) increases by the end of 2030 compared to 2010. Therefore, those extreme rainfall events are expected to influence the occurrence of landslide by the end of 2030.

### 3.2 Slope Modelling

The slope in numerical analysis is divided in two layers. The first layer is sandy silt soil (Fig. 3), and the second layer is sand layer. The soil properties are presented in Table 1. The soil Properties are established as the Initial condition, where the change of soil properties due to rainfall Infiltration is Influenced by $\varphi_b$ (Eq. 1). The internal friction angle ($\varphi'$) is obtained by using the direct shear test. The saturated permeability ($k_s$) is tested by using a constant head. As seen in Fig. 3, the first layer is identified as a sandy silt layer while the second layer is identified as sand layer. The slope has an inclination of approximately 18$^o$. The Y direction of the slope established in roll

joint to model in Y direction movement. On the other side, the X direction of the slope is modelled in pinned joint to illustrates in x and y directions.

### 3.3 Hourly Rainfall Data

To convert the daily rainfall data Into hourly rainfall intensity, a fixed duration is required. In this study, 8 hr of rainfall duration is chosen based on the rainfall threshold established by Prasetyaningtiyas et al. (2024). Three rainfall intensities have been chosen in this study, i.e., 6.46 x $10^{-7}$ m/s, 3.49 x $10^{-7}$ m/s, and 1.246 x $10^{-7}$m/s for December, January and February, respectively. The average rainfall intensity from December 2010 to February 2030 (Fig. 4) is employed and simulated in water unit flux (q) on the slope surface. The unit flux works as load and seepage. In this study, the rainfall mean value indicates the most intense rainfall in February followed by December and the smallest in January.

### 3.4 Slope Stability

At the early stage of slope modeling (steady state), there is no rainfall applied on the slope surface. The model is based on the geometry and the soil condition that is obtained through the soil investigation report. In the next stage, the transient phase, the rainfall is employed on the slope surface. At the end of rainfall, the water flux is recognized as running off, particularly at point A (Fig. 5a). Point A is chosen as the ending point of the main body of slope and the collecting point of runoff of the slope surface. Based on this condition, this point represents the biggest runoff on the slope surface.

As shown in Fig. 5(a), the slip surface is not fully in the main body of the slope with a Factor of Safety (FS) equal to 1.575, categorized as a stable slope (Mahmoodzadeh et al., 2022). In December (Fig.5b), the rainfall is applied which results in a runoff in the end of rainfall up to 0.0268$m^3$ at point A. In this condition, the FS decreased to 1.094. In January (Fig.5c), the runoff reached 0.0205$m^3$. It leads to a higher FS at around 1.19, almost reaching 1.2. As for February forecast (Fig.5d), the rainfall average peaked among all models with an FS dropped to 1.1. However, the February model shows the biggest slip surface among all the other months. It is probably influenced by the amount of rainfall intensity in February. All the models also proved that the slope is not stable under 8 hr of average in the past and future conditions (2010-2030). Based on this condition, the annual slope failure is expected to continue, since the rainfall model is obtained from average rainfall data. In addition, the fact that the maximum rainfall is not applied as a rainfall model increases the probability of worse condition in an existing area.

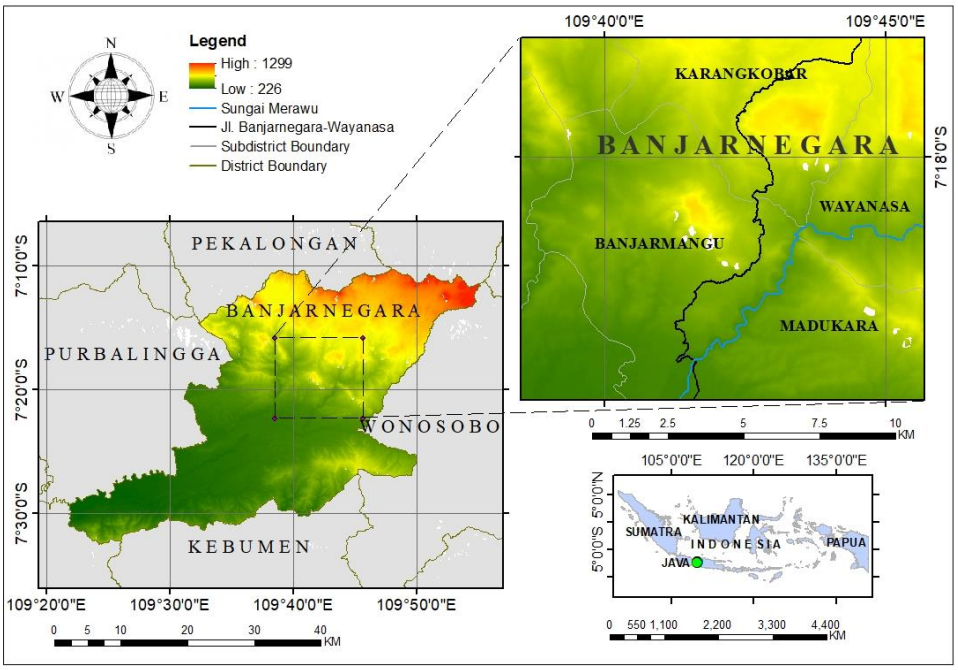


Figure 1. Area of analysis during wet season (DJF) for Paweden and Kalilunjar (area inside the black-dashed box at 7.26°-7.48°S & 109.5°-109.72°E).

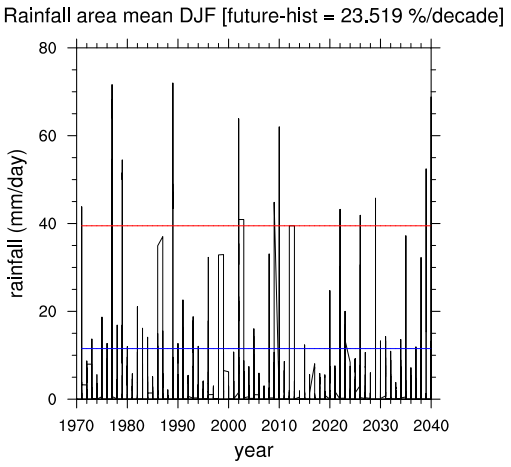


Figure 2. 5-day running mean of the daily rainfall (mm/day) during the wet season (DJF) from 1971-2040 (black line). The line graph represents the area mean inside the black-dashed box in Fig. 1. For reference, the 95$^{th}$ (blue line) and 99$^{th}$ (red line) percentile values are overlayed into the plot. The trend is calculated from the annual mean of daily rainfall value for each period. The trend value is normalized against the mean value and converted to percent per decade.

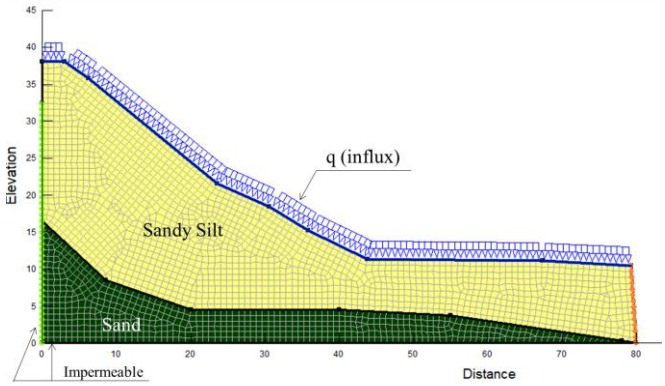


Figure 3. A 2D slope model

Table 1. Soil Properties

| No | Variable | Unit | Value | Soil layer |
|---|---|---|---|---|
| 1 | **Water content (*w*)** | % | 39.67 | Sandy silt |
| 2 | **Cohesion (*c*)** | kg/cm$^2$ | 0.13 | Sandy silt |
| 3 | **Internal friction angle ($\varphi'$)** | $^o$ | 28 | Sandy silt |
| 4 | **Specific gravity (gs)** | - | 2.7 | Sandy silt |
| 5 | **Bulk density ($\gamma_b$)** | gr/cm$^3$ | 1.76 | Sandy silt |
| 6 | **Saturated permeability of vegetated soil ($k_s$)** | (m/s) | 1.2x10$^{-5}$ | Sandy silt |
| 7 | **Water content (*w*)** | % | 32 | Sand |
| 8 | **Cohesion (*c*)** | kg/cm$^2$ | 0.02 | Sand |
| 9 | **Internal friction angle ($\varphi'$)** | $^o$ | 34 | Sand |
| 10 | **Specific gravity (gs)** | | 2.72 | Sand |
| 11 | **Bulk density ($\gamma_b$)** | gr/cm$^3$ | 1.76 | Sand |
| 12 | **Saturated permeability of vegetated soil ($k_s$)** | (m/s) | 1.2x10$^{-5}$ | Sand |

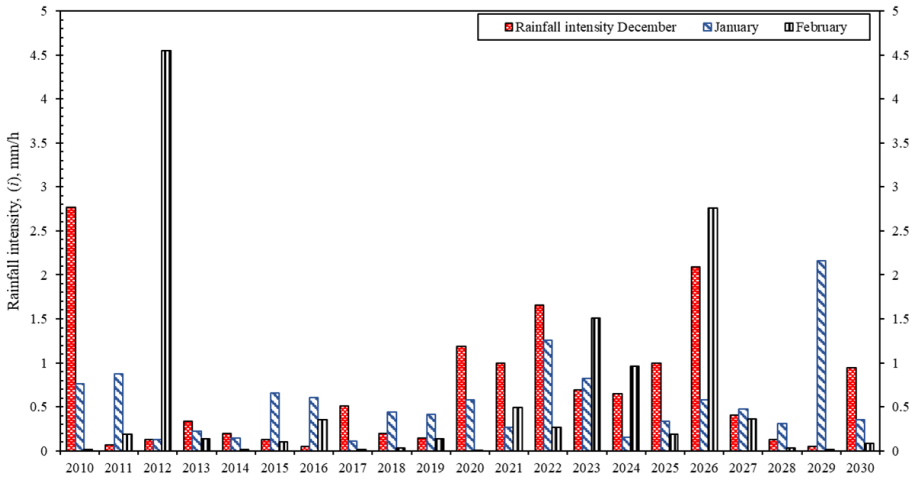


Figure 4. The monthly mean of hourly rainfall data during the rainy season (DJF) converted from the daily CORDEX-SEA dataset.

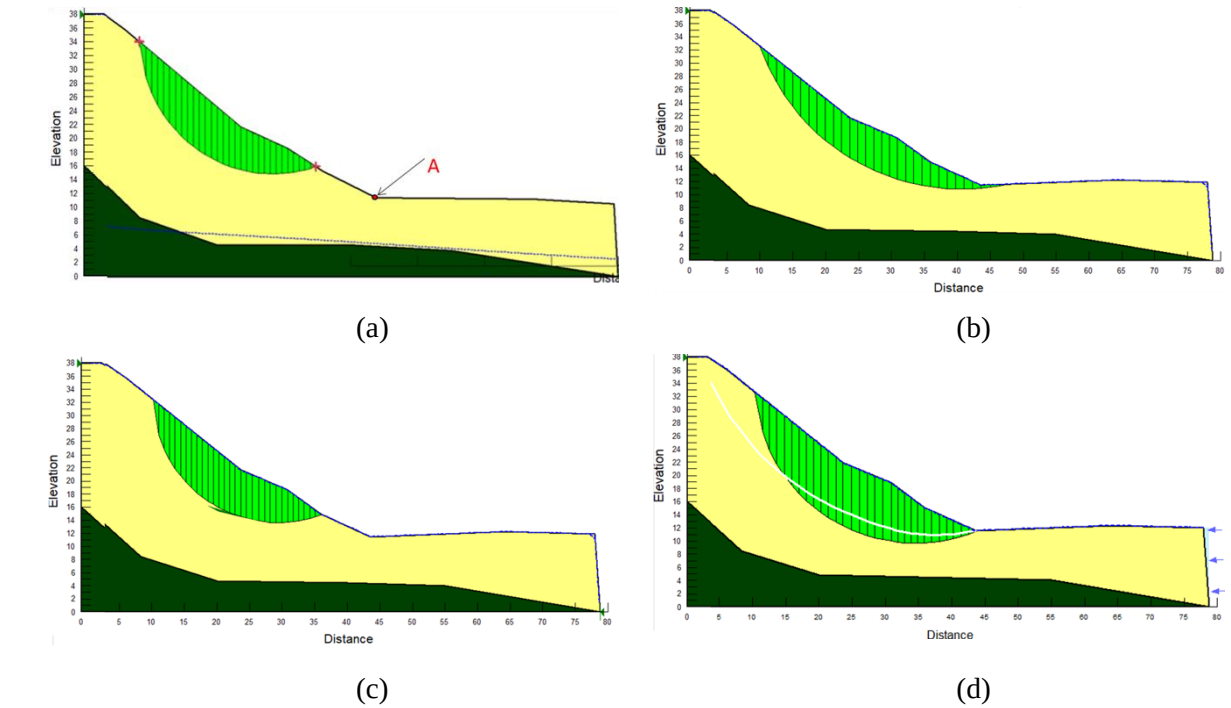


Figure 5. The slip surface of slope (a) in a steady state (FS =1.575) (b) due to December rainfall (FS= 1), (c) due to January rainfall (FS= 1.19), and (d) due to February rainfall (FS= 1.1).

## 4. CONCLUSION

Based on the average of 2010-2030 rainfall dataset, the hourly rainfall model based on the past and future data is established. The rainfall data is then employed as the input of slope stability. All stages of this study results in a few conclusion as follows:

1. CORDEX-SEA model data based on RCA4-CNRM-CM5 shows an increase of occurrence of extreme daily rainfall intensity during the wet season (December-January; DJF) by 2030 in comparison to 2010 condition.
2. The rainfall model shows any slope failure in three months of DJF. It indicates that the annual slope failure is triggered by the rainfall intensity in the wet season.
3. The annual slope failure will remain for the next 5 years from 2025 to 2030. The slope instability is triggered by an average rainfall threshold of 20 years rainfall record.
4. The amount of soil loss based on the slip surface is strongly influenced by the rainfall intensity. In this case, as rainfall is the most intense in February among the other months, it results in the biggest amount of soil mass.

## REFERENCES

Arrisaldi, T., Wilopo, W. & Fathani, T. F. (2021). Landslide Susceptibility Mapping And Their Rainfall Thresholds Model In Tinalah Watershed, Kulon Progo District, Yogyakarta Special Region, Indonesia. Journal Of Applied Geology, 6, 112-118.

Astm-D698 (2003). Standard Practice For Laboratory Compaction Characteristics Of Soil Using Standard Effort (12 400 Ft-Lbf/Ft3 (600 Kn-M/M3)). Book Of Standards 04.08.

Astm (2020). Astm D792-20 (Standard Test Methods For Density And Specific Gravity (Relative Density) Of Plastics By Displacement). United State: Astm.

Astm/D2434-68 (2000). 2434-68 Standard Test Method For Permeability Of Granular Soils (Constant Head) Astm

International. West Conshohocken, Pa.

Astm/D3080 (2012). Standard Test Method For Direct Shear Test Of Soils Under Consolidated Drained Conditions. Book Of Standard, Astm International.

Crozier, M. J. (2010). Deciphering The Effect Of Climate Change On Landslide Activity: A Review. Geomorphology, 124(3-4), 260-267.

Deser, C., Alexander, M. A., Xie, S. P., & Phillips, A. S. (2010). Sea Surface Temperature Variability: Patterns And Mechanisms. 2, 115-143.

Emberson, R., Kirschbaum, D., & Stanley, T. (2021). Global Connections Between El Nino And Landslide Impacts. 12(1), 2262.

Fredlund, D. (1987). Slope Stability Analysis Incorporating The Effect Of Soil Suction. Slope Stability, 113-144.

Giorgi, F., Jones, C., & Asrar, G. R. (2009). Addressing Climate Information Needs At The Regional Level: The Cordex Framework. 58(3), 175.

Held, I. M., & Soden, B. J. (2006). Robust Responses Of The Hydrological Cycle To Global Warming. Journal Of Climate, 19(21), 5686-5699.

Hendrawan, I. G., Asai, K., Triwahyuni, A., & Lestari, D. V. (2019). The Interanual Rainfall Variability In Indonesia Corresponding To El Niño Southern Oscillation And Indian Ocean Dipole. 28, 57-66.

Karnawati, D., Fathani, T., Andayani, B., Burton, P. & Sudarno, I. (2009). Strategic Program For Landslide Disaster Risk Reduction: A Lesson Learned From Central Java, Indonesia. Wit Transactions On The Built Environment, 110.

Laboratory, S. M. (2015). Soil Investigation Report (Banjarnegara-Wanayasa Lane). Diponegoro University.

Lin, Q., Wang, Y., Glade, T., Zhang, J., & Zhang, Y. (2020). Assessing The Spatiotemporal Impact Of Climate Change On Event Rainfall Characteristics Influencing Landslide Occurrences Based On Multiple Gcm Projections In China. 162, 761-779.

Mcgregor, S., Cassou, C., Kosaka, Y., & Phillips, A. S. (2022). Projected Enso Teleconnection Changes In Cmip6. 49(11), E2021gl097511.

Muntohar, A. S., Prasetyaningtiyas, G. A. & Hidayat, R. (2021). The Spatial Model Using Trigrs To Determine Rainfall-Induced Landslides In Banjarnegara, Central Java, Indonesia. Journal Of The Civil Engineering Forum. Petra Christian University, 289-298.

Nguyen, P. L., Bador, M., Alexander, L. V., Lane, T. P., & Ngo-Duc, T. (2022). Nguyen, P. L., Bador, M., Alexander, L. V., Lane, T. P., & Ngo-Duc, T. (2022). More Intense Daily Precipitation In Cordex-Sea Regional Climate Models Than Their Forcing Global Climate Models Over Southeast Asia. 42(12), 6537-6561.

Nguyen-Thanh, H., Ngo-Duc, T., & Herrmann, M. (2023). The Distinct Impacts Of The Two Types Of Enso On Rainfall Variability Over Southeast Asia. 61(5), 2155-2172.

Nikulin, G., Jones, C., Giorgi, F., Asrar, G., Büchner, M., Cerezo-Mota, R., . . . Van Meijgaard, E. (2012). Precipitation Climatology In An Ensemble Of Cordex-Africa Regional Climate Simulations. 25(18), 6057-6078.

Prasetyaningtiyas, G. A., Mase, L. Z., Rifa'i, A., Fathani, T. F., Listyawan, A. B. & Azhom, M. N. (2024). The Influence Of Rainfall Variation On Slope Stability: Case Study Of Wanayasa Street Slope, Banjarnegara, Indonesia. Transportation Infrastructure Geotechnology, 1-19.

Satyaningsih, R., Jetten, V., Ettema, J., Sopaheluwakan, A., Lombardo, L., & Nuryanto, D. E. (2023). Dynamic Rainfall Thresholds For Landslide Early Warning In Progo Catchment, Java, Indonesia. 119(3), 2133-2158.

Weidman, S. (2021). Understanding Changes In Precipitation With Climate Change Over Wet And Dry Land (Doctoral Dissertation, Massachusetts Institute Of Technology).

Yang, T., Ding, J., Liu, D., Wang, X., & Wang, T. (2019). Combined Use Of Multiple Drought Indices For Global Assessment Of Dry Gets Drier And Wet Gets Wetter Paradigm. Journal Of Climate, 32(3), 737-748.

Yun, K. S., Lee, J. Y., Timmermann, A., Stein, K., Stuecker, M. F., Fyfe, J. C., & Chung, E. S. (2021). Increasing Enso–Rainfall Variability Due To Changes In Future Tropical Temperature–Rainfall Relationship. 2(1), 43.

Zaitchik, B. F., Rodell, M., Biasutti, M., & Seneviratne, S. I. (2023). Wetting And Drying Trends Under Climate Change. 1(6), 502-513.